

SURFACE STATES AND EFFECTIVE SURFACE AREA ON **PHOTOLUMINESCENT**  
P-TYPE POROUS SILICON

S.Z. WEISZ, A. RAMIREZ PORRAS, AND O RESTO,

Department of Physics, University of Puerto Rico, Rio Piedras, PR 00931

and

Y. GOLDSTEIN, A. MANY, AND E. SAVIR

Racah Institute of Physics, The Hebrew University, Jerusalem 91904, Israel

## ABSTRACT

The present study is motivated by the possibility of utilizing porous silicon for spectral sensors. Pulse measurements on the porous-Si/electrolyte system are employed to determine the surface effective area and the surface-state density at various stages of the anodization process used to produce the porous material. Such measurements were combined with studies of the photoluminescence spectra. These spectra were found to shift progressively to the blue as a function of anodization time. The luminescence intensity increases initially with anodization time, reaches a maximum and then decreases with further anodization. The surface state density, on the other hand, increases with anodization time from an initial value of  $\sim 2 \times 10^{12} \text{ cm}^{-2}$  for the virgin surface to  $10^{13} \text{ cm}^{-2}$  for the anodized surface. This value is attained already after  $\sim 2 \text{ min}$  anodization and upon further anodization remains fairly constant. In parallel, the effective surface area increases by a factor of 10-30. This behavior is markedly different from the one observed previously for n-type porous Si.

## INTRODUCTION

The work presented here was motivated by the possibility of the use of porous silicon as a spectral sensor. Porous silicon,  $1-4$  (PS) obtained by electrochemical etching procedures applied to crystalline Si surfaces, when illuminated by u.v. light, exhibits high luminescence efficiencies in the visible range. This effect, and the parallel electroluminescence effect, promise the possibility of the realization of PS based optoelectronic devices on top of crystalline silicon. One such possibility is the use of porous silicon on top of silicon charge coupled devices (CCD). Silicon CCD devices are used in many applications of optical imaging. However, the silicon spectral sensitivity is quite limited in the blue and u.v. because of surface recombination. The incorporation of porous silicon into a silicon based imaging system may enable the extension of the spectral range towards the u.v.

The present work concentrates on gaining further insight into the porous silicon photoluminescence process and the role of the surface in this process. To that end we have employed combined studies of the luminescence spectrum, the surface-state density and the effective surface area of the porous surface. Such studies were carried out at different stages of the anodization process and thus for different morphologies of the porous surface. The luminescence spectra were measured by conventional methods. The surface state characteristics and the effective surface area were determined by pulse measurements on the PS/electrolyte system. This system is particularly suitable since a capacitative contact to the terrain of the porous surface is best achieved by an electrolyte, and it was successfully used<sup>6</sup> to investigate n-type PS. There we found<sup>6</sup> a strong correlation between the surface-state density near the conduction band edge and the luminescence intensity. In this paper we present similar measurements on *p-type* porous Si and we compare the results with those obtained on n-type material.

## EXPERIMENTAL

The starting material was high-grade p-type silicon wafers of resistivity in the range 20–50  $\Omega\text{cm}$ . A p<sup>+</sup> layer was formed by diffusing metallic Al into one of the faces to obtain an ohmic contact. The sample was attached to a cylindrical Teflon cell via a Kalrez O-ring, the sample constituting the bottom of the cell, with its free surface facing upwards. The samples were etched in 20°/0 HF. In order to prepare the porous surface,<sup>4</sup> a solution of HF, ethanol and water (1:1 :2) was poured into the cell. A platinum electrode was immersed in the solution and a spring contact was attached to the p<sup>+</sup> contact. The anodization of the Si surface was carried out with a current density of 100 mA/cm<sup>2</sup>.

The luminescence of the PS was excited by a 10 mW He-Cd laser beam ( $\lambda = 442$  rim). The luminescence spectra at different stages of the anodization process were measured by a Control Development spectrometer.

The electronic characteristics of the PS/electrolyte interface were studied at different stages of the anodization process, starting from the “virgin” surface and up to an anodization time of 20 minutes. To that end, the anodizing solution was replaced after each anodization stage by an electrolyte; an aqueous solution of KCl. The measurement technique applied to the semiconductor/electrolyte (WE) interface has been described elsewhere,<sup>5</sup> and will be reviewed only briefly here. A short voltage pulse of duration  $T = 20 \mu\text{sec}$ , applied between the Pt electrode and the sample’s p<sup>+</sup> contact, is used to charge up the interface region. The voltage drop across these electrodes, measured just after the termination of the pulse ( $T + dT$ ), represents to a very good approximation the change  $\delta V_s$  in barrier height across the semiconductor space-charge layer induced by the applied pulse. If an insulating layer, such as an oxide, is present at the semiconductor surface, the measured voltage drop is  $\delta V_s + \delta V_g$ , where  $\delta V_g$  is the drop across the insulating layer. Obviously,  $\delta V_g = Q_{\text{tot}}/C_g$ , where  $Q_{\text{tot}}$  is the total charge density induced at the surface and  $C_g$  is the “geometric” capacitance of the insulating layer (per cm<sup>2</sup>).  $Q_{\text{tot}}$  is obtained from the voltage  $V_c$  developed across a large series capacitor C, again at the termination of the pulse. Pulses of varying amplitude are applied singly, one per data point taken. In this manner possible damage to the porous surface is minimized,

In general,  $Q_{\text{tot}}$  is made up of three components:

$$Q_{\text{tot}} = \delta Q_{\text{sc}} + \delta Q_{\text{ss}} + Q_{\text{L}} , \quad (1)$$

where  $\delta Q_{\text{sc}}$  is the change in the free space-charge density,  $\delta Q_{\text{ss}}$  is the change in surface-state charge density, and  $Q_{\text{L}}$  is the charge density that has leaked across the interface due to imperfect blocking of the S/E interface. In order to determine each component of  $Q_{\text{tot}}$ , the platinum electrode is shorted to ground by an electronic switch at  $T + dT$ , where  $dT$  is very short (O. 1 – 0.2  $\mu\text{sec}$ ), just sufficient to permit accurate readings of  $\delta V_s$  and  $V_c$  right after the termination of the pulse. At this point, charge redistribution between C and the S/E interface begins to take place. In the first stage, the free charge  $\delta Q_{\text{sc}}$  and its equal counterpart in C discharge relatively fast through the low resistance of the sample and the electrolyte. The decay constant associated with this process is typically several microseconds. As a result,  $V_c$  decays to the value  $\delta Q_{\text{ss}}/C$ ,  $\delta Q_{\text{ss}}$  being the charge remaining in C after the fast decay process. Thereafter,  $V_c$  decays to zero usually much more slowly, as charge trapped in the surface states by the charging pulse are thermally re-emitted into the conduction band, in the case of n-type semiconductor, or valence band, in the case of p-type semiconductor. The decay time is larger the farther away the surface states are located energetically from the relevant band edge and the lower the temperature.<sup>7</sup> If charge leakage exists,  $V_c$  does not decay to zero but to the value  $Q_{\text{L}}/C$ . Subsequently it remains practically constant since the leaked charge has been lost from the interface and the remaining charge  $Q_{\text{L}}$  on C cannot be dissipated. This behavior enables the separate determination of the three components in Eq. (1), all as functions of  $\delta V_s$ . In what follows, we shall express these components in terms of hole surface densities:  $\delta P_s = \delta Q_{\text{sc}}/q$  and  $\delta P_{\text{ss}} = \delta Q_{\text{ss}}/q$ , where  $q$  is the absolute magnitude of the electronic charge.

In most cases a space-charge layer already exists at the semiconductor surface, before applying any bias. It is characterized by an equilibrium barrier height  $V_{so}$  and an equilibrium surface hole density  $P_{so}$ . If surface states are present, there may also be an equilibrium density  $P_{SSO}$  of "occupied" surface states.  $V_{so}$  and  $P_{so}$  can be determined quite accurately from measurements in the depletion range.<sup>8</sup> The entire plots of  $P_s$  and  $P_{SS}$  vs.  $V_s$  can then be constructed by using the relations  $V_s = V_{so} + \delta V_s$ ,  $P_s = P_{so} + \delta P_s$ , and  $P_{SS} = P_{SSO} + \delta P_{SS}$ . So much so in the absence of an insulating layer (such as an oxide) at the semiconductor surface. If such a layer is present, the as-measured barrier height, i. e., the measured voltage drop between the Pt electrode and the p<sup>+</sup> contact just after the pulse termination, yields  $V_s + V_g$ , where  $V_g$  is the voltage drop across the insulating layer.

## RESULTS AND DISCUSSION

In Fig. 1 we present typical photoluminescence spectra of p-type PS surfaces prepared by anodization. The different anodization times are marked on the spectra. We notice that the luminescence intensity at the beginning increases with anodization time, attains a maximum and then decreases. This behavior is illustrated by the higher curve in Fig. 2 and is quite similar to that observed<sup>6</sup> previously for n-type PS. The lower curve in Fig. 2 shows the appreciable blue shift of the spectra, suggesting that, on the average, the porous structure gets finer with anodization time.

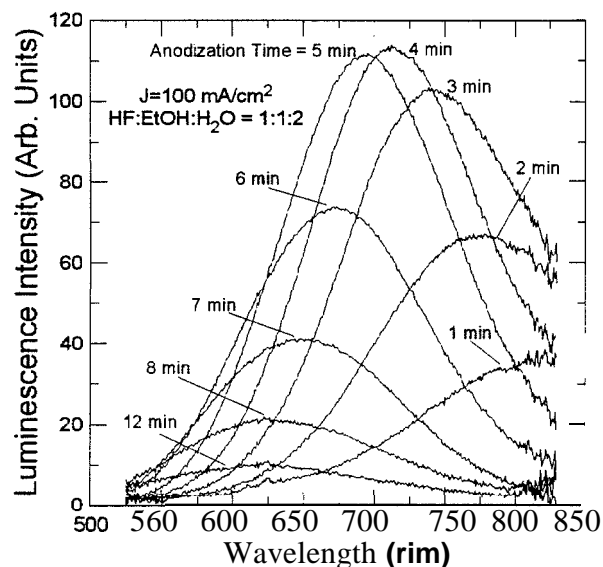


**Fig.1.** Photoluminescence spectra for various anodization times, as marked.

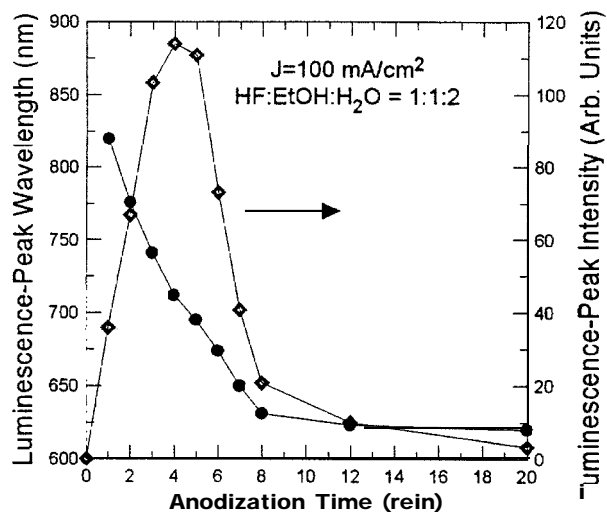


**Fig. 2.** Peak-photoluminescence intensity and wavelength as functions of anodization time for the sample in Fig. 1.

Typical results of the free surface-hole density  $P_s$  (diamonds) and the density of occupied surface states  $P_{SS}$  (stars) against the as-measured barrier height  $V_s + V_g$  as obtained for an etched virgin silicon surface, are displayed in the semilog plot of Fig. 3. In the depletion range,  $P_s$  is negative but, because of the logarithmic scale used, the plot is that of  $-P_s$ . The light curve, in the accumulation range, labeled  $C_g = \infty$ , represents the theoretical dependence of  $P_s$  on  $V_s$  for an oxide-free surface ( $C_g = \infty$ ,  $V_g = 0$ ), as derived from a solution of Poisson's equation for the value of the hole bulk concentration  $p_b$  marked in the figure. It is seen that this curve does not account well for the data in the accumulation range. The best fit, represented by the bold curve, labeled  $C_g = 4.5 \mu F/cm^2$ , was obtained by assuming the presence of an oxide layer of  $C_g = 4.5 \mu F/cm^2$ , corresponding to an oxide thickness of  $\sim 4 \text{ \AA}$ . Again, this behavior is similar to that found on n-type PS. Turning now to the surface-state hole occupancy  $P_{SS}$ , it is seen to rise slowly from a low

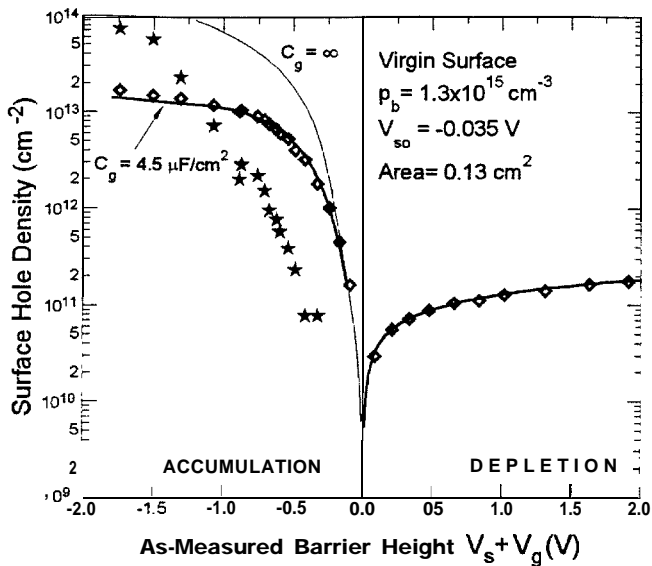


**Fig. 3** Free surface hole density  $P_s$  (diamonds) and density of occupied surface states  $P_{ss}$  (stars) vs. the as-measured barrier height  $V_s+V_g$  for a virgin Si surface. The light and bold curves are theoretical plots of  $P_s$  as explained in the text.

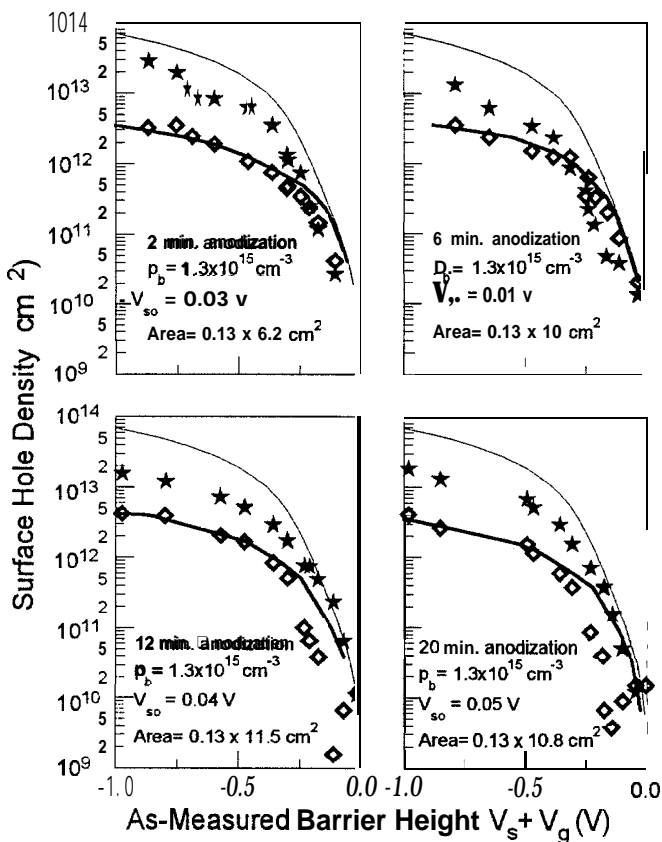


**Fig. 4**  $P_s$  (diamonds) and  $P_{ss}$  (stars) vs.  $V_s+V_g$  for four anodized, porous Si surfaces. The light and bold curves are theoretical plots of  $P_s$ .

value of  $-10^{11} \text{ cm}^{-2}$  at  $V_s+V_g \approx -0.5 \text{ V}$  up to  $\sim 10^{14} \text{ cm}^{-2}$  at  $V_s+V_g \approx -2 \text{ V}$ . No saturation value for the surface-state density could be reached. This is quite different than the behavior we found<sup>6</sup> on n-type PS, where the surface-state density saturated at  $10^{12} \text{ cm}^{-2}$ . Because of this lack of saturation, we shall use the values of  $P_{ss}$  at  $V_s+V_g \approx -1 \text{ V}$  to compare surface state occupancies for different anodization times. For the case of the virgin surface, this value is  $\sim 2 \times 10^{12} \text{ cm}^{-2}$ .

Results of  $P_s$  and  $P_{ss}$ , similar to those in Fig. 3, for four porous surfaces are presented in Fig. 4. These results were obtained after the sample of Fig. 3 has been anodized for different times, as marked in the figure. Since our aim is to compare the surface-state densities, we show only the accumulation range here. Because of the increase of the effective surface area, the highest surface potential barriers (for holes) attained were around -1 volt. The curves in the figure are theoretical, calculated for the same  $C_g$  values as in Fig. 3. We notice again that for all four porous surfaces, the surface-state density (stars) increases monotonously with the potential barrier through the whole region shown and does not exhibit signs of saturation. As mentioned above, we choose for comparison the values of  $P_{ss}$  at  $-1 \text{ V}$ . These values in the figure are scattered around  $2 \times 10^{13} \text{ cm}^{-2}$ , about an order of magnitude higher than on the virgin surface. However, the interesting thing is that this surface-state density remains fairly constant with anodization time, very much different from the results found<sup>6</sup> for n-type PS. A behavior similar to that of the surface states was observed also for the effective surface area. In Fig. 5 the surface area factor, e.g. the ratio of the effective area to the area of the virgin sample, for two typical samples is plotted against the anodization time. The area factors were derived from measurements of the type shown in Figs. 3 and 4. The results for the two samples are qualitatively the same; the area factor increases with anodization time till it reaches a saturation. The saturation values observed varied from sample to sample

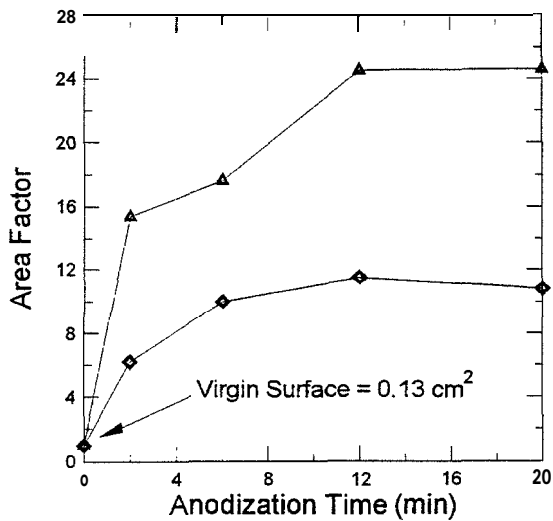


**Fig. 5.** Surface area factor vs. anodization time for two samples.

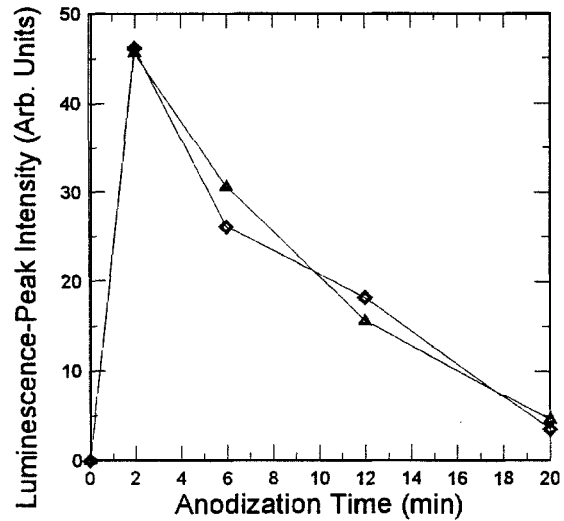


**Fig. 6.** Photoluminescence-peak intensity vs. anodization time for two samples.

between 10 and 30.

In parallel with the **surface-state** density, we measured the **photoluminescence** spectrum for each anodization time. These measurements were performed after the measurements on the PS/electrolyte system. In Fig. 6 the luminescence- peak intensity is plotted against the anodization time for the same two samples as in Fig. 5. We notice that the maximum luminescence peak obtains already after 2 **min** anodization and then the luminescence decreases upon further anodization. In Fig. 7 we plot the value of the luminescence-peak wavelength as a function of anodization time. The peak shifts to the blue upon anodization close to 200 **nm** from its value at 2 **min** anodization.

Comparing the results of Figs. 6 and 7 to those in Fig. 2 we notice that they both show comparable blue shifts, but there is a discrepancy in the anodization time needed to attain maximum luminescence. To check the influence of the **KCl** electrolyte used in the electronic measurements, we measured the spectra on **PS** samples that after anodization were immersed for 10 **min** into a **KCl** electrolyte. The results are shown in Fig. 8 and, for comparison, we also re-

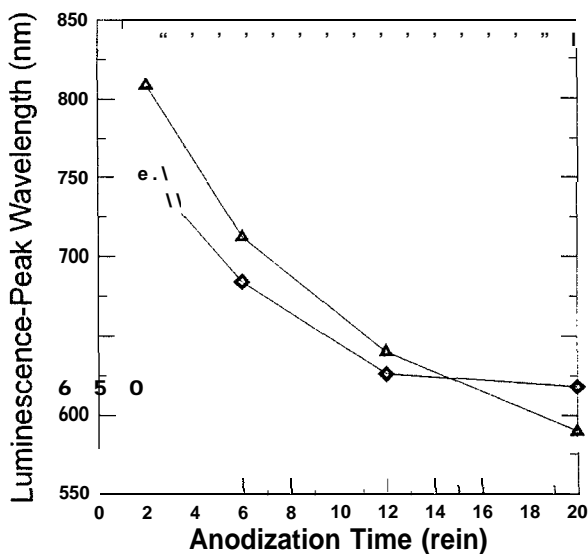


**Fig. 7.** Photoluminescence-peak wavelength vs. anodization time for two samples.

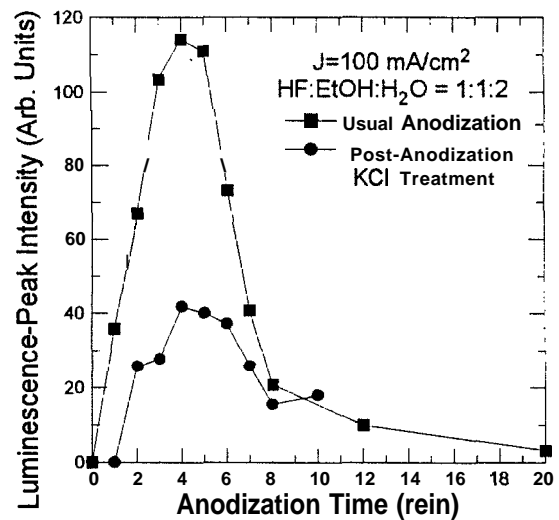


**Fig. 8** Photoluminescence-peak intensity for an untreated and for a **KCl** treated sample vs. anodization time.

plotted the corresponding curve from Fig. 1. We notice that the **KCl** treatment does not **shift** the maximum to a different anodization time, however, it does lower the luminescence intensity. This latter is probably due to adsorption of some species, from the electrolyte. Thus we ascribe the **shift** of the anodization time for maximum luminescence, to possible surface damage due to the application of the voltage pulses.

## CONCLUSION

P-type **PS** behaves quite differently from that of n-type **PS**. While the **photoluminescence** intensity exhibits a pronounced maximum **with** anodization time, the effective surface area and the surface state density appear to reach a more **or** less constant value as a **function** of anodization time. This is in contrast to n-type **PS**, where a close correlation between the effective surface area, the luminescence intensity and the surface-state density was **found**.<sup>6</sup> The discrepancy between the two results can be reconciled once we realize that in both cases the surface states are measured under accumulation conditions. The surface states involved are then those near the majority carrier band edge; namely, near the conduction band for the n-type material and near the valence band for the p-type material. Thus our present **results** suggest that the **surface** states near the valence-band edge are not involved in the luminescence process.

## ACKNOWLEDGMENT

The work in Puerto Rico was supported by NASA grant No. NCCW-0088 and by NSF EPSCoR Grant No. OSR-94-52893, while the work in Israel was supported by the Ministry of Science, Israel, within the framework of the infrastructure-applied physics support project.

## REFERENCES

1. L.T. Canham, *Appl. Phys. Lett.* 57, 1046(1990).
- 2.1. Amato, *Science* 252, 922 (1991).
3. A.G.Cullis and L.T. Canham, *Nature* 353,335 (1991).
4. For the recent developments in this field see: Z.C. Feng and R. Tsu, *Porous Silicon* (World Scientific, Singapore, 1994).
5. M. Wolovelsky, J. Levy, Y. Goldstein, A. Many, S.Z. Weisz and O. Resto, *Surf Sci.* 171,442 (1986).
6. S.Z. Weisz, J. Avalos, M. Gomez, A. Many, Y. Goldstein, and E. Savir in *Defect- and Impurity-Engineered Semiconductors and Devices*, edited by S. Ashok, J. Chevalier, I. Akasaki, N.M. Johnson, and B.L. Sopori (*Mater. Res. Soc. Proc.* 378, Pittsburgh, PA, 1995) pp. 899-904.
7. A. Many, Y. Goldstein, and N.B. Grover, *Semiconductor Surfaces* (North-Holland, Amsterdam, 1971).
8. S.Z. Weisz, J. Penalbert, A. Many, S. Trokman, and Y. Goldstein, *J. Phys. Chem. Solids* 51, 1067 (1990).